# Surface and Interface Characterization of Ferritic Stainless Steel by $^{57}$Fe Conversion Electron Mössbauer Spectroscopy (CEMS)

Kiyoshi Nomura, Takayuki Terai, and Tsuguo Sawada

School of Engineering, The University of Tokyo

Hongo 7-3-1, Bunkyo-ku, Tokyo, 113-8656

The surface and interface on ferritic stainless steel heated at various high temperatures were characterized by Conversion Electron Mössbauer Spectroscopy. The iron oxides ($\alpha$-Fe$_2$O$_3$) were mainly produced by heating below 600$^{\circ}$C and the chromium oxides were produced with fine paramagnetic iron oxides species above 700$^{\circ}$C. The interface of stainless steel beneath the oxide films was especially characterized as the hyperfine field distributions. CEMS is effective for simultaneous and non-destructive characterization of both oxides surface and alloy interface layers of ferritic stainless steel.

## 1. Introduction

Stainless steel is widely used in many fields. However, there are a few applications of oxide films prepared intensively on stainless steel. We have shown that the oxide film of austenitic SUS316 (18Cr+8Ni+3Mo+Fe balance) treated chemically is a practical pH sensor with a quick response [1]. The oxide film on stainless steel heated in advance is useful for vacuum vessels because there is few gas absorption [2]. In addition, ferritic stainless steel (such as SUS430: 18Cr+Fe balance) is one of candidate materials for high-temperature container, heat exchange vessel of nuclear fusion. For example, low activation ferritic stainless steel is expected as the liquid blanket and container material of LiF-BeF$_2$ molten salt, which is considered as a coolant and a breeder material of tritium [3]. The surface study on stainless steel is important.

On the other hand, the oxidized states of iron steel surfaces have been analyzed using conversion electron Mössbauer spectroscopy (CEMS) [4]. There are few applications of CEMS to characterization of oxide surface of stainless steel [5]. After Mössbauer effect of $^{57}$Fe, 7.3 keV K-electrons (80%), 13.6 keV L-electrons (8%) and 5.5 keV auger electrons (63%) are emitted together with the secondary electrons of reemitted 6.3 keV K$\alpha$ X-rays (23%) and 14.4 keV $\gamma$-rays (10%). Although these electrons can be distinguished with high performance electron analyzers such as XPS, the electron spectroscopy with high energy-resolution are not practically so useful for CEMS from the viewpoint of detection efficiency. It is known that the 65% of all conversion electrons emitted from Fe metal is within 60 nm in depth and the 90 % is

within 300 nm in depth [6]. Concerning the interface between coating and substrate steel, we have first reported that the relative intensity ratio between sextet peaks of iron substrate became from 3:4:1:1:4:3 close to 3:2:1:1:2:3 with the increase of dipping time in the phosphated bath [7]. This is mainly caused by the increase of roughness at the interface by the long term of chemical treatment. When analyzed the complex CEMS and XMS spectra of the carbonitride coatings of stainless steel in 1996 [8], we could not find the state transition of the base stainless steel by integral CEMS.

The thin interface of ferritic stainless steel beneath the oxide layers was especially estimated from the hyperfine field distributions of three different energy CEMS spectra by using a He gas proportional counter. As the results, the different hyperfine fields were obtained.

## 2. **Experimental**

Some SUS430 plates were oxidized by heating in air atmosphere for 1 hour at 400, 500, 600, 700, and $800^oC$.   Radiation source used was 1.85GBq $^{57}Co$(Cr). The $\gamma$-rays were perpendicularly irradiated to a sample plane. CEMS spectra were measured using a $2\pi$ back scattering type of gas flow counter, flowing He+5%$CH_4$ gas at 15cc/min and applying high voltage at 950 V. A He gas counter has poor energy and time ($\mu$sec) resolutions, but high efficiency of $2\pi$ stradian to detect all conversion electrons together with the insensitivity against incident $\gamma$ and X rays.   The typical electron energy spectrum is shown in Fig.1.
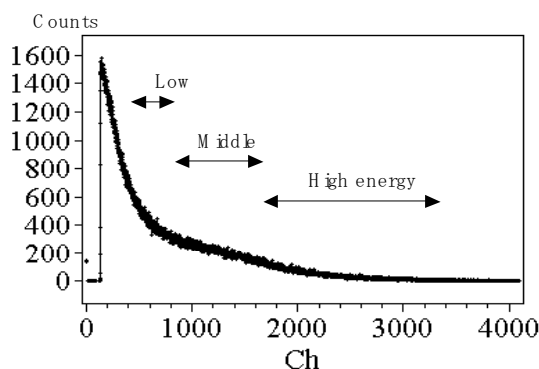


Fig.1 PHA spectrum of conversion electrons detected by a gas flow counter, flowing He+5%$CH_4$ gas at 15 cc/min. HV: 950V, Source: $^{57}Co$ (Cr), Sample: Stainless steel ($^{57}Fe$;2.1%, natural abundance)

Three Mössbauer spectra were simultaneously obtained by discriminating the energy of emitted electrons into three regions such as the high, middle and low energy. This method can provide the rough layer-by-layer analysis within about 100nm. MossWinn program [9] was used for the analysis of CEMS spectra and the hyperfine fields distributions.

3. Results

3.1 Depending of CEMS on different energy electrons detected.

The typical CEMS spectra of the stainless steel (SUS430) heated at 500°C for 1 hour are shown in Fig.2. Three spectra were simultaneously obtained by discriminating three different electron energy regions. It was found that a magnetic sextet ($H_{in}$=52T) observed is assigned to an antiferromagnetic iron product of hematite ($\alpha$-$Fe_2O_3$). The higher contents of hematite produced at the top layers were observed in CEMS spectra obtained by detecting the higher energy electrons. It was confirmed that the rough layer-by-layer analysis by a gas counter is possible. CEMS spectra obtained by the detection of low energy electrons were not so good for the peaks to back grounds.   It is why many non-resonant secondary electrons due to photoelectron effect and Compton effect contribute to low energy regions.

The sextet of the original ferritic stainless steel consisted of broad peaks because the iron internal magnetic fields were influenced due to the various numbers of nearest neighbor Cr atoms around an Fe atom. These broad peaks were analyzed using an internal magnetic field distribution by the method of Hesse and Rubartsch [10].   Since the direction of magnetic moment is parallel in-plane in the most thin surface of ferromagnetic materials such as an iron foil, the area intensity ratio between sextet peaks becomes 3:4:1:1:4:3 for γ-ray vertical incidence. However, the internal magnetic field distributions were analyzed assuming that the magnetic splitting components in the surface region observed by integral CEMS had average intensity ratio of 3:3:1:1:3:3 because the best fitting of Mössbauer spectrum of non-treated sample was obtained using this ratio. As shown in the right figures of Fig. 2, it is clear that the internal magnetic field distributions of the stainless steel substrate were strongly affected by discriminating the electron energy. The peaks of 270 and 310 kOe were observed in the hyperfine distributions of high energy CEMS although the peak of hyperfine field distributions was 290 kOe before treatment as shown in Fig.3a). The distributions in low energy regions became similar to that before treatment. Those results suggest that the composition ratio of Fe and Cr is different from that of the bulk at the near interface layers beneath the oxides layers. It is known that the magnetic phase diagram of Fe-Cr alloy consists of a ferromagnetic component for Fe concentration in excess of 19 at.% [11]. The elemental Fe and Cr have similar lattice structures of BCC with close lattice constants, and the local magnetic moment of Fe and Cr depends on their local environment of Cr next neighbors rather than the average electric properties. In the ferromagnetic region, the average local moment is reduced when the Fe-Cr coupling is ferromagnetic, although the Fe local moment increases slightly when the coupling is

antiferromagnetic [12]. It is known that the magnetic hyperfine field at the Fe site decreases with the decrease of Fe concentration [13, 14].
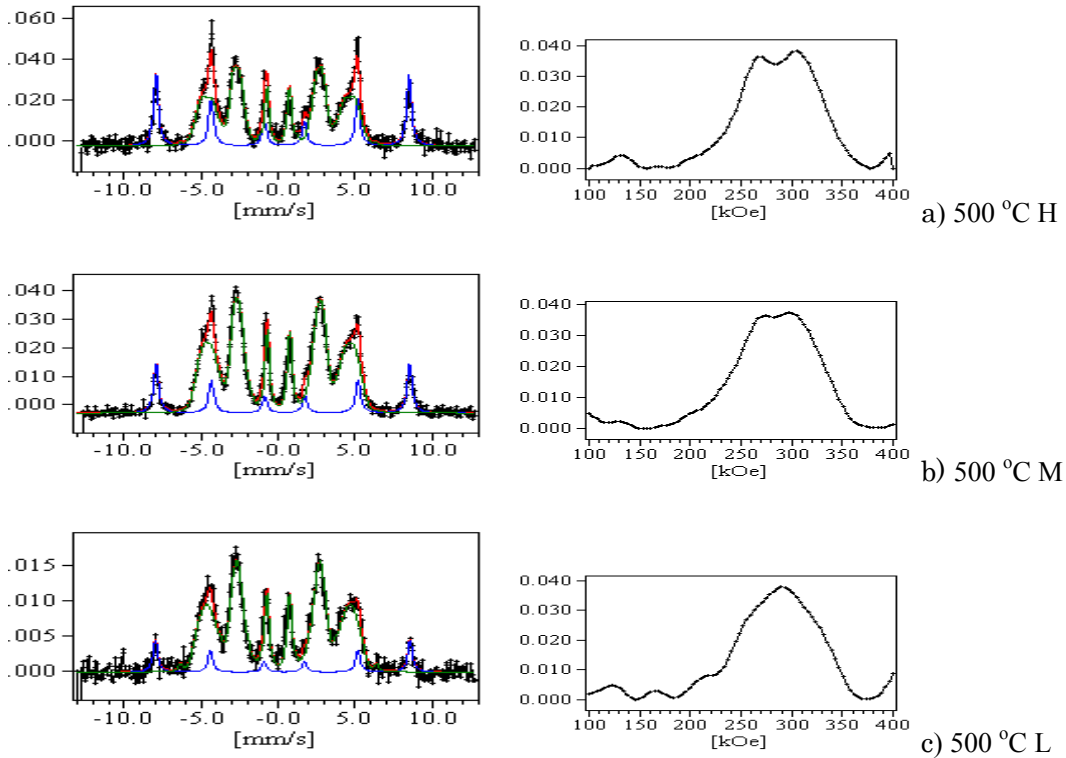

a) 500 °C H


b) 500 °C M


c) 500 °C L

Fig. 2 CEMS and hyperfine distributions of SUS430 heated at 500°C for 1 hour. a) high energy electrons, b) middle energy electrons, and c) low energy electrons detected.

## 3.2   Temperature dependence on oxide surface and interface layers

Fig.3 shows CEMS spectra of the stainless steel heated at various temperatures, which were obtained by addition of high energy CEMS to middle energy CEMS spectra. The peak at 33T with relatively high intensity was observed in the hyperfine magnetic field distribution of the sample oxidized at 700°C. This indicates that the chromium depletion occurs at the interface of the substrate beneath oxide layers. In the hyperfine field distribution of the sample oxidized at 800°C, the peak at 33T became low again, and lay close to the original hyperfine field distribution. It means that the composition at the substrate interface approximates the original bulk composition of SUS430 with the diffusion of bulk Cr atoms to the interface to form Cr oxide surface layers at the higher temperatures. It was found that Cr depleted layer could be detected by CEMS measurement of the interface of stainless steel heated at high temperatures.

From the relative peak intensity ratio of iron oxides and stainless substrate, it was found that iron atoms were diffused to form top oxide layers up to 600°C and chromium

oxides were grown in the top oxide layers at 700°C or higher. At 800°C, the intensity of hematite became small, and the paramagnetic peaks with IS=0.33mm/s, QS=0.33mm/s were observed. This is reduced in the small particles of hematite or $(Cr,Fe)_2O_3$ doped with Cr.
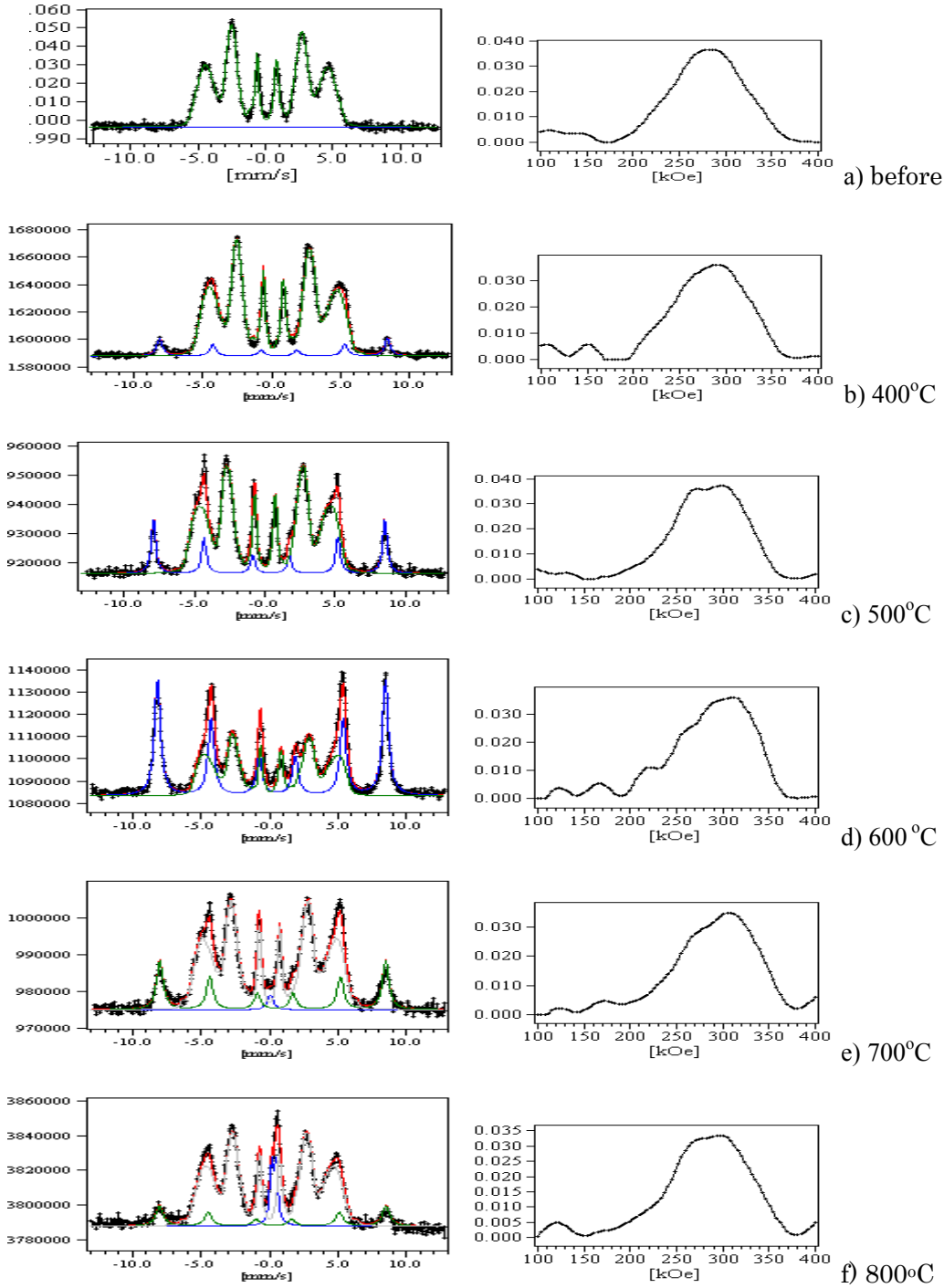


a) before

b) 400°C

c) 500°C

d) 600 °C

e) 700°C

f) 800°C

Fig.3　CEMS and hyperfine distributions of SUS430 heated at various temperatures for 1 hour in air. a) before and after heating b) 400°C, c) 500°C. d) 600°C, e) 700°C and f) 800°C.

The schematic diagram of the oxide layers produced on stainless steel and the probing depth by detecting low, middle, and high energy CEMS are shown in Fig.4.
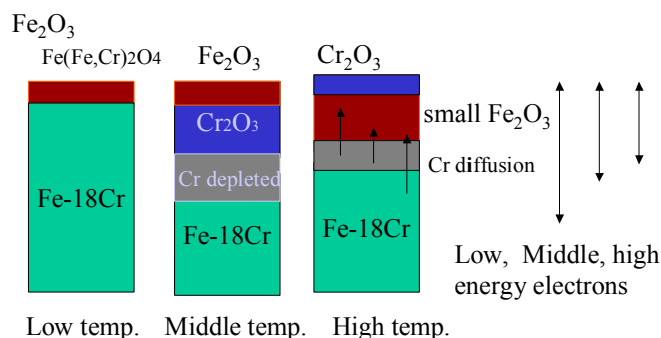


Fig. 4, Schematic cross sections of oxide layers produced on ferritic stainless steel and the detection depth by three different energy CEMS.

## 3. Conclusions

Depth selective CEMS by a He gas flow counter could not only determine the iron products on steel surface within about 100nm but also simultaneously detect the degradation of composition of Cr and Fe in the interface substrate beneath the surface products by analysis of the magnetic hyperfine distributions.

Reference

1) K. Nomura, and Y. Ujihira, *Analytical Chemistry*, **60**(1988) 2564.

2) B. Cho, E. Choi, S. Chung, K. Kim, T. Kang, C.park, B.Kim, *Surface Science*, 439(1999)L799.

3) K. Nomura, Y. Hosoya, H.Nishimura, T. Terai, *Czechoslovakia J. of Phys.*, 2001 , in press.

4) K. Nomura, Y. Ujihira, A. Vertes, *J. Radioanaly. and Nucl. Chem., Articles*, **202**(1996) 103.

5) K. Nomura, Y. Ujihira, *J. Materials Science*, **25** (1990) 1745.

6) I. Stwert, M.J.Tricher, Corrosion Science, **26**(1986) 1041.

7) K. Nomura, Y. Ujihira, Y.Matsushima, R. Koshima, Y.Sugawara, *Jap. J. of Chem.*, 1372 (1980).

8) K. Kurosawa, M. Hoshino, H.Li, Y. Ujihira, K. Nomura, *Hyperf. Interact.*, **112**(1998) 269.

9) Z. Klencsar, E. Kuzmann, A.Vertes, *Hyperf. Interact.*, **202**(1996) 103.

10) J. Hesse, A. Rubartsch, *J. Phys. E: Science Instruments*, **7** (1974) 526.

11) V.I.Anisimov, V.P.Antrov, A.I.Liechtenstein, V.A.Gubanov, A.V.Postnikov, *Phys. Rev.* B**37** (1988) 5598.

12) M.E.Elzain, J. Phys. *Condes. Matter*, **3**(1991) 2089.

13) H. Kuwano, K. Ono, *J. Phys. Soc. Japan*, **42**(1977) 72.

14) M. Shiga, and Y. Nakamura, *J. Phys. Soc. Japan*, **49**(1980) 528.